Published in final edited form as: IEEE Trans Biomed Eng, Vol. 63, No. 4, pp. 797-804, Apr. 2016. doi:10.1109/TBME.2015.2474131
Code available from: http://www.mathworks.com/matlabcentral/fileexchange/53326-cvxeda

cvxEDA: a Convex Optimization Approach to Electrodermal Activity Processing

Alberto Greco, *Student Member, IEEE*, Gaetano Valenza, *Member, IEEE*, Antonio Lanata, *Member, IEEE*, Enzo Pasquale Scilingo, *Member, IEEE*, and Luca Citi*, *Member, IEEE*

***Abstract*—*Goal:* This paper reports on a novel algorithm for the analysis of electrodermal activity (EDA) using methods of convex optimization. EDA can be considered one of the most common observation channels of sympathetic nervous system activity, and manifests itself as a change in electrical properties of the skin, such as skin conductance (SC). *Methods:* The proposed model describes SC as the sum of three terms: the phasic component, the tonic component, and an additive white Gaussian noise term incorporating model prediction errors as well as measurement errors and artifacts. This model is physiologically inspired and fully explains EDA through a rigorous methodology based on Bayesian statistics, mathematical convex optimization and sparsity. *Results:* The algorithm was evaluated in three different experimental sessions to test its robustness to noise, its ability to separate and identify stimulus inputs, and its capability of properly describing the activity of the autonomic nervous system in response to strong affective stimulation. *Significance:* Results are very encouraging, showing good performance of the proposed method and suggesting promising future applicability, e.g., in the field of affective computing.**

***Index Terms*—Convex optimization, electrodermal activity, skin conductance, sparse deconvolution.**

I. INTRODUCTION

ELECTRODERMAL activity (EDA) broadly refers to any alteration in the electrical properties of the skin. One of the most frequently used measures of EDA is skin conductance (SC). Electrodermal signals are a manifestation of the activity in eccrine sweat glands that are innervated by the sympathetic branch of the autonomic nervous system (ANS), mainly by the sudomotor nerves [1]. Indeed, when the sudomotor nerves stimulate the production of sweat, the conductivity measured on the skin surface changes as a result of sweat secretion and of variations in ionic permeability of sweat gland membranes [2]–[4]. Although sweating is primarily a means of thermoregulation, sweat glands located on the palmar and plantar (glabrous) surfaces possibly evolved to increase grip and enhance sensitivity, and may be more responsive to psychologically significant stimuli than to thermal ones [2], [4]. This relationship between EDA, ANS, and psychological stimuli — together with the relative ease of measurement — makes this physiological signal widely popular in neuroscience research, including information processing, quantification of arousal levels during emotional and cognitive processes, and clinical research examining predictors and correlates of normal and pathological behaviour [5]–[7].

The SC signal can be decomposed in two components, tonic and phasic, which have different time scales and relationships to the triggering stimuli. Tonic phenomena include slow drifts of the baseline skin conductance level (SCL) and spontaneous fluctuations (SF) in SC [4]. The phasic component, skin conductance response (SCR), reflects the short-time response to the stimulus. The typical shape of the SCR comprises a relatively rapid rise from the conductance level followed by a slower, asymptotic exponential decay back to the baseline.

When the interstimulus interval (ISI), i.e. the temporal gap between two consecutive stimuli, is shorter than the recovery time of the first response, the two SCRs overlap. This occurrence is observed in many experimental paradigms, particularly in cognitive neuroscience where common values of ISI (1–2 s) are generally shorter than the recommended minimum ISI to avoid such an overlap, which is around 10–20 s [5], [8]. The overlap issue is probably the main limitation in a set of factors regarding the decomposition of SC into its phasic and tonic components. Despite the wide use of EDA measurements, the generation of SCR via skin sympathetic nerve fibres remains an understudied topic.

In the past two decades, several mathematical solutions have been developed to decompose the phasic signal into individual SCRs associated to each stimulus, even during short ISI experimental paradigms, and to model how ANS activity (and, in particular, the sudomotor nerve activity) causes SCRs. This process allows estimation of ANS activity with potentially better time resolution than using the raw SCR signal. Many of the early methods, whose primary aim was to overcome the overlap issue, required visual inspection and introduced subjective elements into the analysis. For example, Barry *et al.* [9] attempted to correct the baseline by subtracting each SCR from an extension of the preceding SCR using graphical tools. Lim *et al.* [10] instead proposed a model based on a response function made of 4–8 parameters optimized for each single response to obtain a response-by-response variation in SCR shape. This method also required visual inspection to select the best model.

Further automation of the analysis occurred through the description of the peripheral system as a linear time-invariant (LTI) system and the development of different classes of mod-

The research leading to these results has received partial funding from the European Union Seventh Framework Programme FP7/2007-2013 under grant agreement n 601165 of the project WEARHAP and from the School of computer science and electronic engineering, University of Essex. *Asterisk indicates corresponding author.*

A. Greco and *L. Citi are with the School of Computer Science and Electronic Engineering, University of Essex, Colchester CO4 3SQ, UK (corresponding author email: lciti@ieee.org).

A. Greco, A. Lanata, G. Valenza, and E. P. Scilingo are with Department of Information Engineering and Research Center "E. Piaggio", Faculty of Engineering, University of Pisa, Pisa, Italy.

els based on this assumption [11]. In addition to decomposing the phasic signal into individual SCRs, these models often attempt to estimate the ANS activity by searching for the most likely input signal which could explain the observed output (the measured SC). The first LTI model was presented by Alexander *et al.* [12]. Their method permits the estimation of the sudomotor nerve activity (SMNA) using a model where the SC is the result of a convolution between discrete bursting episodes of the SMNA and a biexponential impulse response function (IRF) assumed known a priori and time invariant.

Benedek and Kaernbach criticized some aspects of Alexander's model and developed two new models in which the LTI assumption was modified to take into account the variability in SCR shape. These methods are known as non-negative deconvolution [13] and continuous deconvolution analysis (CDA) [14]. Both models split the SMNA into two parts, one describing the phasic activity and the other representing EDA variations of different origins (e.g., noise). Both models assume a pharmacokinetic model of the dynamic law of diffusion of sweat. They adopted a biexponential IRF, called the Bateman function. Although observation noise is not formally modelled in any of these methods [12]–[14], all of three assume its existence. They estimate a noisy SMNA and then recover a filtered phasic component using a low-pass filter and a subsequent heuristic and prefixed peak-detection scheme.

Recently, Bach *et al.* presented the SCRalyze toolbox (now incorporated into PsPM), which comprises several models that assume a linear time-invariant system [15]. These models and that of Alexander *et al.* use a heuristic IRF whose parameters have been optimized on large datasets. SCRalyze algorithms try to estimate the model input (SMNA) or parameters that best explain the observed SC data based on optimization methods. Moreover, they include a noise term, which also accounts for possible violations of the assumption of time invariance.

Using several aspects of these previously assessed methodological approaches (e.g., the IRF), our previous study [16] proposed decomposing SC signals into smooth tonic and sparse phasic components through the solution of a convex optimization problem. The solution of the problem incorporated the physiological knowledge about EDA by means of an appropriate choice of constraints and regularizers. In particular, the non-negativity of the SMNA — that [14] promoted using a soft penalty — was seamlessly enforced by our previous (and current) model through the use of a non-negative constraint on the corresponding optimization variable. More recently, Chaspari *et al.* [17] also proposed a sparse representation of EDA but their use of overcomplete dictionaries leads to a non-convex problem with no guarantee of finding the globally optimal solution. Since an amazing variety of practical problems can be cast in the form of a convex optimization problem, mathematical optimization has become an important tool in many disciplines and the list of its applications is steadily growing [18].

In this paper, we present a novel method to estimate the ANS activity from the EDA using a convex optimization approach. The model is grounded on Bayesian statistics and a simple yet physiologically sound representation of the observed SC as the sum of three components: a slow tonic component; the output of the convolution between an IRF and a sparse (compact, bursty) non-negative SMNA phasic driver; and an additive noise term. We model the IRF — which is related to the phasic component — as an infinite impulse response (IIR) function by means of an ARMA model. Compared to a finite impulse response (FIR) or matched filter approach, the IIR system exhibits better accuracy (by not requiring truncation of the IRF) and greater computational efficiency, thanks to a more compact representation of the system. After introducing the method in Section II, we report the results of a thorough evaluation of the algorithm on simulated and real data. Experimental results, described in Section IV, demonstrate the model's positive attributes, also through a comparison with the CDA [14], which has been of great inspiration for this study.

II. ALGORITHM

A. Convex Optimization

The goal of an optimization problem,

$$\begin{aligned} &\text{minimize } f_0(x) \\ &\text{subj. to } f_i(x) \leq 0 \quad i = 1, \ldots, m, \end{aligned} \tag{1}$$

is to find the best possible choice among the vectors belonging to the subset of $\mathbb{R}^n$ defined by the constraint functions. An optimization problem is convex when both the objective and the constraint functions are convex [18]. In the context of mathematical optimization, the most important consequence of convexity is that necessary conditions for local optimality are also sufficient for global optimality. In other words, if a convex function is minimized, the global optimal value of the problem will always be found. Contrary to most nonconvex problems, for some important categories of convex optimization problems, there are algorithms that can reliably and efficiently solve very large-scale problems. A special subclass of convex optimization problems is represented by quadratic optimization (quadratic program, QP) wherein the objective function is a quadratic polynomial in the variables and the constraints are all affine functions [18]. The cost function of a QP may include l^2-norm and l^1-norm regularization terms that can be used to prevent overfitting or to favour sparse solutions, i.e. solutions with a large number of components equal to zero. We will show now that, given a set of physiologically sound assumptions, the EDA deconvolution problem can be cast as a quadratic optimization problem.

B. Model Assumptions

We modelled the EDA generation process based on the following assumptions:

- $\mathcal{A}1$) SCRs are preceded by bursts from the sudomotor nerves controlling the sweat glands. These bursts are temporally discrete episodes [19], [20], i.e. SCRs are generated by a neural signal that is sparse and non-negative because of the nature of a nerve activity.
- $\mathcal{A}2$) The relationship between the number of sweat glands recruited and the amplitude of a firing burst is linear [20]. Moreover, the output response of the system depends

only on the instant where the nerve input is applied. Stated otherwise, the timecourse of a single SCR induced by a neural burst is not influenced by previous ones, even when their SCRs overlap [21]. In the light of these considerations it is reasonable to characterize the system as linear time-invariant.

$\mathcal{A}3$) The sweat diffusion process has a subject-specific impulse response function (IRF) which is relatively stable for all SCRs from the same subject [14].

$\mathcal{A}4$) This phasic activity is superimposed to a slowly varying tonic activity with spectrum below $0.05\,\text{Hz}$ [22], i.e. whose information content can be represented by samples spaced every $10\,\text{s}$ (e.g., by 10-s averages in [4]).

C. Observation Model

We model a given N-sample long SC signal (y) as the sum of a tonic (t) and a phasic (r) component plus an additive noise term (ϵ):

$$y = r + t + \epsilon, \tag{2}$$

where y, t, r, and ϵ are N-long column vectors. The noise term ϵ is an iid (independent and identically distributed) sequence of zero-average Gaussian random variables with variance σ^2, representing measurement and modelling errors.

The tonic component is represented as the sum of cubic B-spline functions with equally-spaced knots every $10\,\text{s}$ (assumption $\mathcal{A}4$), an offset and a linear trend term:

$$t = B\ell + Cd, \tag{3}$$

where B is a tall matrix whose columns are cubic B-spline basis functions, ℓ is the vector of spline coefficients, C is a $N\times 2$ matrix with $C_{i,1} = 1$ and $C_{i,2} = i/N$, d is a 2×1 vector with the offset and slope coefficients for the linear trend.

Within r, the shape of a single phasic response (under assumptions $\mathcal{A}2$ and $\mathcal{A}3$) is modelled using a biexponential impulse response function, called the Bateman function:

$$h(\tau) = (e^{-\frac{\tau}{\tau_0}} - e^{-\frac{\tau}{\tau_1}})\, u(\tau), \tag{4}$$

where τ_0 and τ_1 are, respectively, the slow and fast time constants while $u(\tau)$ is the unitary step function. The Bateman function is the output of a bi-compartmental pharmacokinetic model representing the diffusion of the sweat through the gland ducts [23]. The Laplace transform of (4) is simply:

$$\mathcal{L}\{h(\tau)\} = \frac{1}{s+\tau_0^{-1}} - \frac{1}{s+\tau_1^{-1}}, \tag{5}$$

where $-\tau_0^{-1}$ and $-\tau_1^{-1}$ are the poles of this second-order LTI system. Its discrete-time approximation, obtained using central differencing (bilinear transform) $s = \frac{2}{\delta}\frac{z-1}{z+1}$ with sampling interval δ, is the following ARMA model:

$$\begin{aligned} H(z) &= \frac{\left(1+z^{-1}\right)^2}{\psi + \theta z^{-1} + \zeta z^{-2}} \\ \psi &= (\tau_1^{-1}\delta + 2)(\tau_0^{-1}\delta + 2)/(\tau_1^{-1}\delta^2 - \tau_0^{-1}\delta^2) \\ \theta &= (2\,\tau_1^{-1}\tau_0^{-1}\delta^2 - 8)/(\tau_1^{-1}\delta^2 - \tau_0^{-1}\delta^2) \\ \zeta &= (\tau_1^{-1}\delta - 2)(\tau_0^{-1}\delta - 2)/(\tau_1^{-1}\delta^2 - \tau_0^{-1}\delta^2). \end{aligned} \tag{6}$$

The ARMA cascade can be represented in matrix form as:

$$q = A^{-1}\,p, \quad r = M\,q, \tag{7}$$

where: p represents the sudomotor nerve activity; q is an auxiliary variable that will be used to find p indirectly; M is a tridiagonal matrix with elements $M_{i,i} = M_{i,i-2} = 1$, $M_{i,i-1} = 2$, $3 \le i \le N$; and A is a tridiagonal matrix with elements $A_{i,i} = \psi$, $A_{i,i-1} = \theta$, $A_{i,i-2} = \zeta$, $3 \le i \le N$.

Finally, the observation model (2) can be written as:

$$y = Mq + B\ell + Cd + \epsilon. \tag{8}$$

D. Maximum a Posteriori Estimation

Given the observation model (8), the goal is to identify the maximum a posteriori (MAP) spike train (p) and tonic component (t) parametrized by $[q, \ell, d]$, for the measured SC signal (y):

$$[q, \ell, d] = \arg\max_{q,\ell,d} P[q, \ell, d \mid y]. \tag{9}$$

Assuming independence between q, ℓ and d (i.e. between the phasic activity, the slowly varying tonic component and the drift) and applying Bayes' theorem, we obtain:

$$P[q, \ell, d \mid y] \propto P[y \mid q, \ell, d]\, P[q]\, P[\ell]\, P[d], \tag{10}$$

where $P[y \mid q, \ell, d]$ is the likelihood of observing a specific SC time series given the parameters of the model, while $P[q]$, $P[\ell]$ and $P[d]$ are the prior probabilities of the parameters. We omitted the evidence $P[y]$ since it plays no role in the optimization. Unlike other approaches in the literature, our model relies exclusively on the presence and definition of the priors in (10) — which we are about to describe in detail — to impose physiologically sound constraints on the signals to be estimated. As a result, the method does not require pre-processing of the observed SC signal (e.g., bandpass filtering) nor post-processing of the inferred phasic and tonic components (e.g., to deal with negative neural activations).

To model the sudomotor nerve activity (p) representing the input ($\mathcal{A}1$) to the LTI system, we use the simplest first order description of spike trains [24], i.e. a Poisson distribution: $p_i \sim \text{Pois}(\lambda\delta)$, where $\lambda\delta$ is the expected firing rate per bin, i.e. λ is the average number of spikes per unit time. To keep the analysis tractable, we replace the Poisson distribution with an exponential distribution of the same mean [24]. In this way the constraint $p_i \in \mathbb{N}$ can be relaxed to $p_i \ge 0$. Finally, since p and q are related by (7), the prior $P[q]$ becomes:

$$P[q] = \prod_{i=1}^{N} \frac{1}{\lambda\delta} e^{-\frac{p_i}{\lambda\delta}} \propto \prod_{i=1}^{N} \exp\left(-(\lambda\delta)^{-1}\,(Aq)_i\right). \tag{11}$$

Concerning the tonic component, we make use of assumption $\mathcal{A}4$ and consider a uniform frequency spectrum in the band $0 - 0.05\,\text{Hz}$. Because we use equally-spaced knots every $\Delta = 10\,\text{s}$, the sampling frequency is exactly twice the upper band limit and the elements of the vector ℓ can be assumed iid. In particular, we adopt a normal distribution for the amplitude at each knot $\ell_i \sim \mathcal{N}(0, \sigma_\ell^2)$. As a result the prior $P[\ell]$ is:

$$P[\ell] = \prod_{i=1}^{Q} \frac{1}{\sqrt{2\pi}\,\sigma_\ell} \exp\left(-\frac{1}{2}\frac{\ell_i^2}{\sigma_\ell^2}\right), \tag{12}$$

where Q is the number of knots (approximately $N\delta/\Delta$). Finally, for the drift coefficients d we assume uninformative priors and drop $P[d]$ altogether from further analysis.

The likelihood term follows immediately from (8) and from the error model $\epsilon \sim \mathcal{N}(0, \sigma^2)$:

$$P[y \,|\, q,\ell,d] = \prod_{i=1}^{N} \frac{1}{\sqrt{2\pi}\sigma} \exp\left(-\frac{(Mq+B\ell+Cd-y)_i^2}{2\sigma^2} \right). \quad (13)$$

Replacing (11), (12) and (13) in (10) and taking the logarithm:

$$\ln P[q, \ell, d \mid y] = -\frac{1}{2\sigma^2} \sum_{i=1}^{N} (Mq + B\ell + Cd - y)_i^2 - \frac{1}{\lambda\delta} \sum_{i=1}^{N} (Aq)_i - \frac{1}{2\sigma_\ell^2} \sum_{i=1}^{Q} \ell_i^2 + \text{const}, \quad (14)$$

with $(Aq)_i \geq 0$. Maximizing (14) yields the MAP solution to (9). After multiplying by σ^2 and substituting $\alpha = \sigma^2/(\lambda\delta)$ and $\gamma = \sigma^2/\sigma_\ell^2$, we rewrite (14) as a constrained minimization problem in matrix form to obtain a more compact notation. This optimization problem, that we term cvxEDA, represents the core of the algorithm presented in this manuscript:

$$\begin{aligned} &\text{minimize } \frac{1}{2} \|Mq + B\ell + Cd - y\|_2^2 + \alpha \|Aq\|_1 + \frac{\gamma}{2} \|\ell\|_2^2 \\ &\text{subj. to } Aq \geq 0. \end{aligned} \quad (15)$$

After some matrix algebra, this optimization problem can be re-written in the standard QP form and solved efficiently using one of the many sparse-QP solvers available. After finding the optimal $[q, \ell, d]$, the tonic component t can be derived from (3) while the sudomotor nerve activity driving the phasic component can be easily found as $p = Aq$.

Although solving (15) is strictly equivalent to maximizing (14), the former has a different interpretation. In the optimization problem, the objective function to be minimized is a quadratic measure of misfit between the predicted and the observed data. Prior knowledge is accounted for by means of additive regularizing terms. For example, the spiking nature of the driving input (assumption $\mathcal{A}1$) is enforced by means of the l^1-norm penalization which is an effective way to sparsify a signal while maintaining convexity [25]–[27]. Smoothness of the tonic curve (assumption $\mathcal{A}4$) is enforced by the choice of the basis (B) and through the l^2-norm penalization of the spline coefficients. The two parameters α and γ control the strength of the penalty for the phasic and tonic components, respectively. A large α (stronger l^1 regularization of p) yields a sparser estimate with most noise-induced spurious spikes suppressed but also more signal distortion (i.e. attenuation of genuine activations). Conversely, a small α produces a less distorted but noisier solution. Concerning γ, higher values mean a stronger penalization of ℓ, i.e. a smoother tonic curve.

III. MATERIALS AND METHODS

There is no universally accepted protocol for the validation of EDA analysis algorithms. A characterization in terms of sensitivity and specificity, as typically done in a pattern recognition framework, is not directly applicable in this context since there is no one-to-one correspondence between external stimuli supposed to elicit ANS responses and skin conductance responses (see [11] for a discussion). Unless the sympathetic nerve activity is also recorded through microneurography, failure to detect a phasic SC response after the occurrence of an experimental stimulus may be equally ascribed to a low sensitivity of the algorithm under study or, alternatively, to the inability of the stimulus to consistently elicit a phasic response. Similarly, detection of phasic activity in the absence of stimulation may be caused by electrodermal changes that are not stimulus-elicited but spontaneous and non-specific, possibly a result of muscular contractions or respiratory irregularities [4]. We tested our new model taking into account evaluation procedures reported in the literature. We first validated the model's ability to estimate phasic and tonic components explaining the observed SC through simulated and experimental data (see "Experiment 1" below). In the latter case, we used a forced maximal expiration task, that a previous study [28] has shown to reliably induce a sympathetic activation. A further validation was performed to investigate the predictive power of features derived from our model in inferring central (mental/emotional) states ("Experiment 2"). In this case, performances of our model were also compared with those obtained from the continuous deconvolution analysis (CDA), as implemented in the Ledalab software [14].

A. Simulated Data

Each simulated SC time series lasted $T = 90\,\text{s}$ and was generated as the sum of three terms: the first one, representing the phasic component of the EDA, was obtained as the result of a convolution between a simulated SMNA and a biexponential IRF ($\tau_1 = 0.7\,\text{s}$, $\tau_0 \sim \text{Unif}(2.0, 4.0)\,\text{s}$); the second one was a slowly varying signal representing the tonic component, obtained as a linear trend plus a sinusoid with a period $T_\text{t} \sim \text{Unif}(45.0, 90.0)\,\text{s}$; the third term was an additive white Gaussian noise (AWGN). The sudomotor nerve activity driving the phasic component was simulated by placing 10 pulses of unit area (modelling neural bursts) at random times with a minimum 1-s distance between them and from the two ends. To test the ability of the method to recover partially overlapping SCRs in the presence of noise, two sets of 100 time series were generated with different levels of signal-to-noise ratio (SNR): 33 dB and 13 dB (defined as $10\log_{10}(a^2/\sigma_\text{N}^2)$ where a is the foot to peak amplitude of a single SCR and σ_N^2 is the AWGN variance).

B. Experiment 1

In the first experiment, 15 healthy subjects (aged 18–35 years; 7 females) performed a forced maximal expiration task [28], in which they were asked to breathe out with the maximum possible intensity in order to trigger the ANS-mediated expiration reflex. All subjects gave written informed consent prior to taking part in the study, which was approved by the local Ethics Committee. A Biosemi Active II system was used to acquire the SC signal and the respiratory effort (by means of a thoracic respiration belt). The protocol started with the subjects breathing normally and resting in front of a grey monitor for three minutes in order to record their

TABLE I
AROUSAL RATING OF IAPS IMAGES USED

Session	Arousal rating	Arousal range	Arousal level
N	2.81 ± 0.24	$2.42 - 3.22$	VL
A1	3.58 ± 0.30	$3.08 - 3.98$	L
A2	4.60 ± 0.31	$4.00 - 4.99$	L-M
A3	5.55 ± 0.28	$5.01 - 6.21$	M-H
A4	6.50 ± 0.33	$5.78 - 6.99$	H

baseline levels. This was followed by three stimulus sessions in which subjects had to perform a deep expiration whenever the colour of the screen background changed to black. Each session consisted of six forced expirations with a variable ISI chosen randomly among 4, 8 and $12\,$s. Consecutive sessions were separated by a 30-s recovery interval.

This experimental paradigm was chosen to obtain SC signals in which the presence of an autonomic response to the stimulus was as objective and reliable as possible. In fact, previous studies have shown that the forced expiration protocol is a valid method of evoking SCRs unaffected by emotional change with more stable waveform patterns, less habituation and better reproducibility than other means of stimulation (including electrical) [28]. In this way, the presence of at least one SCR after each stimulus was ascertained, allowing determination whether the new methodological approach was able to separate and identify each phasic response even when stimuli were close to each other and their SCRs overlapped.

C. Experiment 2

In the second experiment, 15 healthy subjects (aged 22–26 years; 7 female) different from the previous ones were stimulated by viewing affective images from the official IAPS database [29] to assess our algorithm's predictive validity, i.e. its ability to distinguish stimulations with different arousal content and provide meaningful information about ANS activation. All subjects gave written informed consent before taking part in the study, which was approved by the local Ethics Committee. Subject were comfortably seated in an acoustically insulated room watching the slideshow on a computer screen while their SC was recorded using a BIOPAC MP150 physiological acquisition system. The affective elicitation consisted of four arousal sessions alternated with four neutral sessions: N, A1, N, A2, N, A3, N, A4; where N sessions are sequences of 6 very low arousal (VL) images while Ai (with $1 \leq i \leq 4$) are sets of 20 images eliciting increasing levels of arousal. Details about arousal rating values are reported in Table I. Arousal sessions were classified as Low (L), Low–Medium (L–M), Medium–High (M–H) and High (H) according to the IAPS score criteria. Each image was presented for $10\,$s.

D. EDA Processing and Analysis

For each dataset, the convex-optimization-based EDA model (cvxEDA) described in Section II was applied to each SC time series. As per assumption $\mathcal{A}3$, a subject-specific IRF was considered for this study. While $\tau_1 = 0.7\,$s was used for all subjects, the optimal τ_0 was determined on a per-subject basis as the value $\tau_0 \in [2.0, 4.0]\,$s that minimized the l^2-norm of the residual after fitting the cvxEDA model. Fixed values $\alpha = 0.0008$ and $\gamma = 0.01$, chosen during previous exploratory tests on separate data, were employed throughout this analysis.

The accuracy of the algorithm on the simulated dataset was assessed by measuring its ability to recover the neural activations in the phasic driver from noisy SC time series. For each time series, the set of occurrence times $\mathcal{T}^{\mathrm{e}}$ of pulses with area exceeding a 0.5 threshold was compared to the set of times $\mathcal{T}^{\mathrm{s}}$ of the impulses in the original simulated SMNA using an algorithm modelled after the AAMI/ANSI EC38:1998 standard. Briefly, times in $\mathcal{T}^{\mathrm{e}}$ and times in $\mathcal{T}^{\mathrm{s}}$ were considered as "matching" if they were within a match window of $\pm 0.15\,$s. Each impulse from either signal could only match a single impulse from the other one. Times in $\mathcal{T}^{\mathrm{e}}$ not matching any element of $\mathcal{T}^{\mathrm{s}}$ were considered false positives (FP) while times in $\mathcal{T}^{\mathrm{s}}$ not matching any element of $\mathcal{T}^{\mathrm{e}}$ were considered false negatives (FN). Finally, the performance of the algorithm was measured in terms of sensitivity, computed as the fraction of matched elements of $\mathcal{T}^{\mathrm{s}}$, and positive predictive value (PPV), computed as the fraction of matched elements of $\mathcal{T}^{\mathrm{e}}$.

In the respiratory stimulation dataset, the presence of an estimated burst of SMNA activity was verified in each 5-s time window following a stimulus onset, in order to prove the model's ability to correctly detect real SCRs.

In the last study, to verify that the recovered components represented meaningful information regarding ANS activity, we investigated whether the amplitude of the phasic driver p increased in response to affective stimulation with increasing levels of arousal, as previously reported in the literature [30], [31], [4, ch 3.2.2]. An intersubject analysis compared the responses to the four arousal levels through a non-parametric Page test [32, ch 7.2], under the alternative hypothesis of increasing phasic responses with increasing levels of arousal (we used non-parametric tests because the hypothesis of Gaussianity was rejected by a Kolmogorov–Smirnov test, $p < 0.05$). In post-hoc analysis, each pair of arousal sessions was compared using a one-tailed Wilcoxon signed-rank test with Bonferroni correction to determine significant differences between arousal levels in the expected direction. We computed the adjusted p-value, i.e. the original p-value multiplied by 6 (the number of pairwise comparisons among 4 conditions), to allow direct comparison to the standard significance levels (e.g., 0.05). In the following, we also report the Z-scores (from which the measure of effect size $Z_N = Z/\sqrt{N}$ can be computed, where $N = 15$ is the sample size). Finally, the slow tonic component was analyzed comparing mean values of each arousal session with the preceding neutral session, using a one-tailed Wilcoxon signed-rank test.

IV. RESULTS

For all EDA datasets analyzed, the cvxEDA model produced the expected results: the SC data (Fig. 1(a)) was decomposed into two signals, a sparse component p and a smooth component t, that we interpret as the activity of the sudomotor nerve (Fig. 1(b)) and the tonic level (Fig. 1(c)).

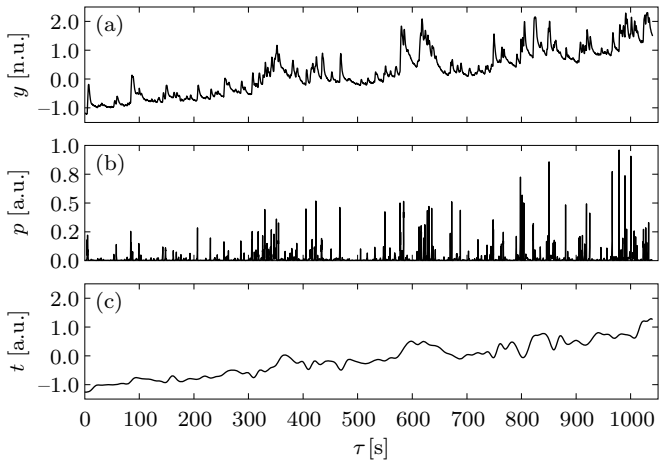

Fig. 1. Application of the cvxEDA decomposition procedure to the SC signal recorded during the forced maximal expiration task for a representative subject. (a) Raw SC signal, Z-score normalized. (b) Estimated sparse phasic driver component p. (c) Estimated slow tonic component t.

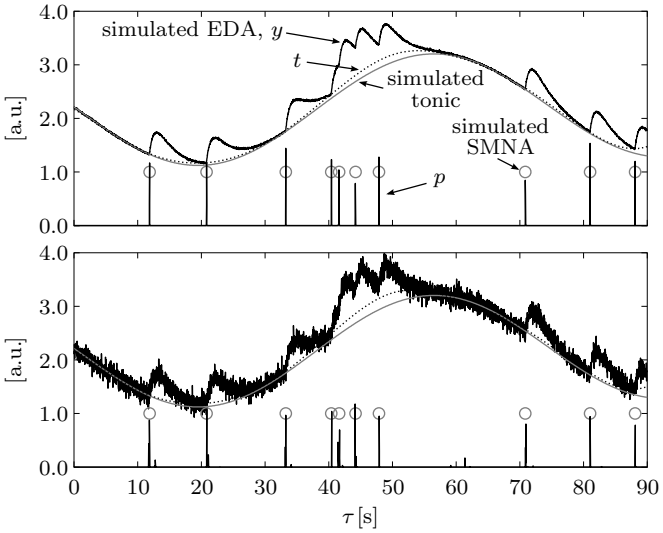

Fig. 2. Solution of EDAcvx model applied to the same simulated signal with different levels of additive white Gaussian noise (top: 33 dB; bottom: 13 dB).

A. Simulated-Data Results

Application of the model to the simulated dataset highlighted the sparsity of the p term as well as the smoothness of the tonic component, even with low SNR. Qualitative visual analysis of Fig. 2 was sufficient to determine that the algorithm worked properly on these data. A quantitative proof was provided in terms of detection performance in recovering the neural activations in the phasic driver from the noisy SC time series. In the high-SNR test the algorithm achieved 99.3% sensitivity and 100.0% PPV on average, whereas it scored 96.7% sensitivity and 91.3% PPV in the low-SNR condition.

B. Experiment 1 Results

Visual inspection of time series recorded during the forced maximal expiration protocol confirmed the effectiveness of the paradigm in eliciting strong SCRs that were partly overlapped

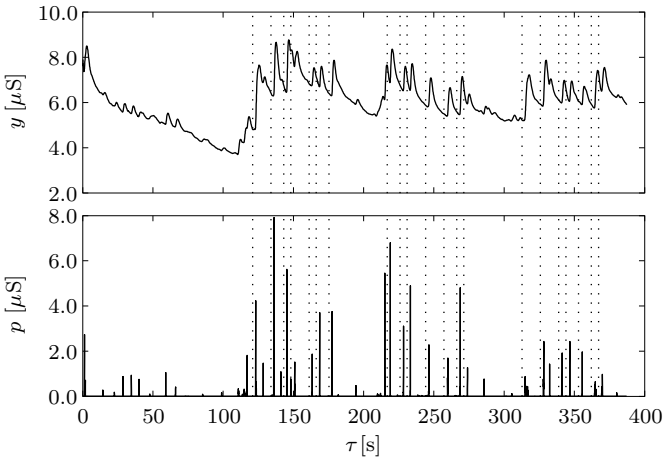

Fig. 3. Example of SC raw data (top) and its estimated phasic component (bottom) during the forced maximal expiration task. Dotted lines mark the onset of the visual cue triggering a forced expiration.

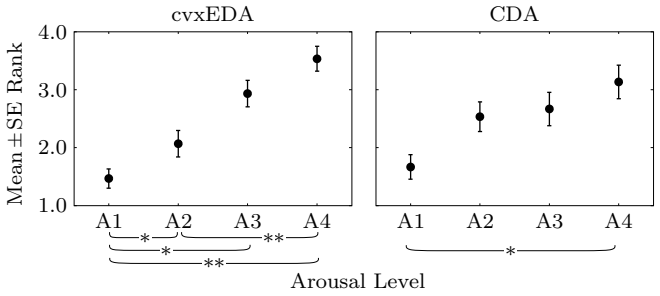

Fig. 4. Within-subject ranks of the peak amplitudes of the phasic component obtained by cvxEDA (left) and CDA (right) for the four arousal levels. The dots mark the across-subject average rank for each level while the wiskers indicate the standard error. The hypothesized effect of arousal level on the phasic component was confirmed by the Page test ($p = 10^{-6}$ for cvxEDA, $p = 0.001$ for CDA). Post-hoc Bonferroni-corrected pair-wise comparisons of the peak amplitudes found significant differences in the cases indicated by asterisks ($*: p < 0.05$; $**: p < 0.01$).

because of short ISIs (Fig. 3). After applying our algorithm, we monitored peaks in the p signal within a 5-s time window post-stimulus (considering the latency of a typical SCR [4]). Intersubject analysis indicated that the algorithm was able to identify the corresponding phasic peak after 96.6% of the stimuli and overcome the overlap issue. Furthermore, visual inspection of the raw SC data in the time windows after stimuli that were not identified by the algorithm showed the almost complete absence of a SCR, probably because of incorrect performance of the task by the subject.

C. Experiment 2 Results

Statistical analysis of the tonic and phasic driver components confirmed the ability of the algorithm to characterize the ANS activity. Page-test results comparing the four arousal sessions indicated a strong significant ($p = 10^{-6}$, $L = 428$, $L^* = 4.74$) relationship between the arousal level and the phasic driver peak amplitude (see also Fig. 4(left)), which is the most appropriate parameter to quantify ANS activity [4]. Post-hoc Bonferroni-corrected pair-wise comparisons revealed significantly larger phasic responses to A2 than to A1 ($p =$

0.040, $Z = 2.47$), to A3 than to A1 ($p = 0.018$, $Z = 2.75$), to A4 than to A1 ($p = 0.002$, $Z = 3.32$), and to A4 than to A2 ($p = 0.004$, $Z = 3.21$). Concerning the tonic component, the Wilcoxon test showed that the tonic mean values were significantly higher during arousal than during neutral sessions ($p = 0.001$, $Z = 3.147$, $Z_N = 0.813$). For comparison, the recordings were also processed using Ledalab, which implements the CDA [14]. This method also decomposes the EDA signal into tonic and phasic components. Consistently with the literature and with results from our cvxEDA model, CDA estimated a phasic driver whose peak amplitude within each arousal session increased with increasing levels of arousal (Page test $p = 0.001$, $L = 409$, $L^* = 3.04$). However, a post-hoc analysis revealed a significant difference ($p = 0.010$, $Z = 2.93$) only between the most extreme sessions, A4 and A1 (see Fig. 4(right)). Overall, our approach provides a stronger correlation and augmented discriminant power, with respect to the elicited arousing session, than CDA.

V. DISCUSSION

In this study, we present a novel algorithm for the analysis of EDA based on maximum a posteriori probability, convex optimization, and sparsity. The model describes the recorded SC as the sum of three terms: the phasic component, the tonic component, and an additive white Gaussian noise term incorporating model prediction errors as well as measurement errors and artifacts. Compared to our previous convex-optimization approach to EDA analysis [16], the new algorithm models the IRF (4) as an ARMA model (i.e. an IIR filter) instead of a MA model (i.e. a FIR filter). This allows a much more compact representation of the IRF by means of two tridiagonal matrices instead of a banded matrix, thus increasing the accuracy and significantly reducing the computational cost. In fact, the sparsity and structure of the problem (15) can be effectively exploited by state-of-the-art sparse-QP solvers. The main difference between our model and established methods in the literature lies in the presence and definition of the prior probabilities for the phasic and tonic signals. Positiveness and burstiness of the sudomotor nerve activity driving the phasic component is modelled through a first order description of spike trains, i.e. assuming a Poisson distribution approximated by an exponential distribution. This form of the prior probability translates into a non-negative inequality constraint and an l^1-norm regularizer in the final optimization problem. Although one could impose a stronger regularization — e.g., l^0-"norm" [27] — on the phasic driver, this would render the problem non-convex, i.e. computationally more demanding, and would significantly deviate from the physiological explanation in terms of Poisson spike trains. Physiologically-plausible temporal scale and smoothness of the tonic input signal are achieved by means of an adequate choice of the spacing between the knots of the spline and through a Gaussian prior on the values at the knots, which ultimately translates into an l^2 regularization of the spline's coefficients in the optimization problem. Thanks to the ARMA observation model and to this choice of priors, we can impose physiologically sound constraints on the signals to be estimated and yet be able to obtain the globally optimal solution by solving a standard quadratic-programming problem. Our proposed cvxEDA model shares some major limitations with most state-of-the-art algorithms, mainly by relying on the strong assumptions of linearity and time-invariance of the system. In reality, physiological systems — especially those involving neural dynamics — are likely to show nonlinear and complex dynamics. Furthermore, such a dynamics and its statistical properties can be different among subjects and further depend on environmental and experimental conditions. Within the proposed EDA modelling framework, inter- and intra-subject variability can be accounted for by choosing a customized IRF function for each subject/condition. This problem was partially addressed in our experimental analysis by performing an outer optimization step to tune the slow time constant of the IRF for each specific subject.

The new algorithm was evaluated in three ways to test its robustness to noise, its ability to separate and identify each phasic response (even when they overlapped because of short ISIs) and its capability of properly describing the activity of the autonomic nervous system in response to strong affective stimulation. The results of the three analyses confirmed the proprieties of the model. On a simulated dataset, the algorithm proved to be robust to different levels of noise. When applied to real data from a forced maximal expiration protocol, the algorithm demonstrated strong ability to reliably detect phasic responses to eliciting stimuli, also overcoming the problem of overlapping SCRs encountered in experimental paradigms involving short ISIs. In the affective stimulation paradigm, the mean tonic level estimated by the model was significantly different in arousal and neutral sessions. Analysing the phasic response, we found a consistent statistical relationship between the arousal levels and the peak amplitude of the estimated phasic driver, thus confirming the model's predictive validity. These results were compared to those obtained using Ledalab's implementation of the CDA [14], a method that performs a deterministic inversion of the peripheral model. The trends found using the CDA confirmed those obtained from our model. However, CDA only found statistically significant differences between the lightest and the strongest levels of arousal while our model allowed a finer discrimination.

Because it can be implemented in few lines of code and does not depend on external libraries (except a conventional QP solver), our algorithm has a wide applicability and can be readily integrated in existing open-source psychophysiological modelling software. Given also the low computational cost of the proposed algorithm, we envisage employing our cvxEDA model in further affective computing applications, including porting the algorithm to wearable/portable monitoring devices (e.g., Empatica tools [33]).

VI. CONCLUSIONS

These encouraging results confirm that our EDA algorithm based on MAP and convex optimization provides a decomposition of the EDA that is robust to noise, overcomes the issue of overlapping SCRs, and provides a window on the ANS activity. Moreover, the solution incorporates the physiological characteristic of the phasic and tonic components by means

of priors and constraints, without requiring pre- or post-processing steps. Another advantage of casting our model as a convex optimization problem is that, once the problem is formalized, a globally optimal solution can be efficiently found using existing solvers. The applicability of our model is not limited to EDA analysis but can be extended to other domains requiring the deconvolution of pulse trains from the output of systems that can be represented as ARMA models, for example in calcium imaging [24] or hormone secretion analysis [27].

REFERENCES

[1] D. Fowles *et al.*, "Publication recommendations for electrodermal measurements," *Psychophysiology*, vol. 18, no. 3, pp. 232–239, 1981.

[2] R. Edelberg, "Electrical activity of the skin: Its measurement and uses in psychophysiology," in *Handbook of psychophysiology*, N. S. Greenfield and R. A. Sternbach, Eds. Holt, Rinehart & Winston, 1972, ch. 9.

[3] ——, "Electrodermal mechanisms: A critique of the two-effector hypothesis and a proposed replacement," in *Progress in electrodermal research*, J.-C. Roy *et al.*, Eds. Springer, 1993, pp. 7–29.

[4] W. Boucsein, *Electrodermal activity*, 2nd ed. Springer Science & Business Media, 2012.

[5] M. E. Dawson, A. M. Schell, and D. L. Filion, "The electrodermal system," in *Handbook of psychophysiology*, J. T. Cacioppo *et al.*, Eds. Cambridge University Press, 2007, ch. 7.

[6] A. Greco *et al.*, "On the deconvolution analysis of electrodermal activity in bipolar patients." in *Proc. 34th Int. Conf. IEEE EMBS (EMBC)*, 2012, pp. 6691–6694.

[7] ——, "Electrodermal activity in bipolar patients during affective elicitation," *IEEE J. Biomed. Health Inform.*, vol. 18, no. 6, pp. 1865–1873, 2014.

[8] A. Breska, K. Maoz, and G. Ben-Shakhar, "Interstimulus intervals for skin conductance response measurement," *Psychophysiology*, vol. 48, no. 4, pp. 437–440, 2011.

[9] R. J. Barry *et al.*, "Elicitation and habituation of the electrodermal orienting response in a short interstimulus interval paradigm," *Int. J. Psychophysiol.*, vol. 15, no. 3, pp. 247–253, 1993.

[10] C. L. Lim *et al.*, "Decomposing skin conductance into tonic and phasic components," *Int. J. Psychophysiol.*, vol. 25, no. 2, pp. 97–109, 1997.

[11] D. R. Bach and K. J. Friston, "Model-based analysis of skin conductance responses: Towards causal models in psychophysiology," *Psychophysiology*, vol. 50, no. 1, pp. 15–22, 2013.

[12] D. Alexander *et al.*, "Separating individual skin conductance responses in a short interstimulus-interval paradigm," *J. Neurosci. Methods*, vol. 146, no. 1, pp. 116–123, 2005.

[13] M. Benedek and C. Kaernbach, "Decomposition of skin conductance data by means of nonnegative deconvolution," *Psychophysiology*, vol. 47, no. 4, pp. 647–658, 2010.

[14] ——, "A continuous measure of phasic electrodermal activity," *J. Neurosci. Methods*, vol. 190, no. 1, pp. 80–91, 2010.

[15] D. R. Bach, "A head-to-head comparison of SCRalyze and Ledalab, two model-based methods for skin conductance analysis," *Biol. Psychol.*, vol. 103, pp. 63–68, 2014.

[16] A. Greco *et al.*, "Electrodermal activity processing: A convex optimization approach," in *Proc. 36th Int. Conf. IEEE EMBS (EMBC)*, 2014, pp. 2290–2293.

[17] T. Chaspari *et al.*, "Sparse representation of electrodermal activity with knowledge-driven dictionaries," *IEEE Trans. Biomed. Eng.*, vol. 62, no. 3, pp. 960–971, 2015.

[18] S. P. Boyd and L. Vandenberghe, *Convex optimization*. Cambridge university press, 2004.

[19] V. G. Macefield and B. G. Wallin, "The discharge behaviour of single sympathetic neurones supplying human sweat glands," *J. Auton. Nerv. Syst.*, vol. 61, no. 3, pp. 277–286, 1996.

[20] T. Nishiyama *et al.*, "Irregular activation of individual sweat glands in human sole observed by a videomicroscopy," *Auton. Neurosci.*, vol. 88, no. 1, pp. 117–126, 2001.

[21] D. R. Bach *et al.*, "Modelling event-related skin conductance responses," *Int. J. Psychophysiol.*, vol. 75, no. 3, pp. 349–356, 2010.

[22] D. R. Bach, K. J. Friston, and R. J. Dolan, "An improved algorithm for model-based analysis of evoked skin conductance responses," *Biol. Psychol.*, vol. 94, no. 3, pp. 490–497, 2013.

[23] R. Schneider, "A mathematical model of human skin conductance," *Psychophysiology*, vol. 24, no. 5, p. 610, 1987.

[24] J. T. Vogelstein *et al.*, "Fast nonnegative deconvolution for spike train inference from population calcium imaging," *J. Neurophysiol.*, vol. 104, no. 6, pp. 3691–3704, 2010.

[25] M. S. O'Brien, A. N. Sinclair, and S. M. Kramer, "Recovery of a sparse spike time series by L1 norm deconvolution," *IEEE Trans. Signal Processing*, vol. 42, no. 12, pp. 3353–3365, 1994.

[26] R. Tibshirani, "Regression shrinkage and selection via the LASSO," *J. R. Stat. Soc. Series B*, pp. 267–288, 1996.

[27] J. de Rooi and P. Eilers, "Deconvolution of pulse trains with the L0 penalty," *Anal. Chim. Acta*, vol. 705, no. 1, pp. 218–226, 2011.

[28] Y. Kira *et al.*, "Sympathetic skin response evoked by respiratory stimulation as a measure of sympathetic function." *Clin. Neurophysiol.*, vol. 112, no. 5, pp. 861–865, 2001.

[29] P. Lang, M. Bradley, and B. Cuthbert, "International affective picture system (IAPS): Digitized photographs, instruction manual and affective ratings," University of Florida, Tech. Rep. A-6, 2005.

[30] E. W. Cook *et al.*, "Affective individual differences and startle reflex modulation." *J. Abnorm. Psychol.*, vol. 100, no. 1, p. 5, 1991.

[31] P. J. Lang *et al.*, "Looking at pictures: Affective, facial, visceral, and behavioral reactions," *Psychophysiology*, vol. 30, pp. 261–261, 1993.

[32] M. Hollander, D. A. Wolfe, and E. Chicken, *Nonparametric statistical methods*. John Wiley & Sons, 2014.

[33] "Empatica: Human data in real time," https://www.empatica.com/.

Alberto Greco (S'13) received the master degree in biomedical engineering from the University of Pisa, Pisa, Italy, in 2010. He is currently a Ph.D. student in automation, robotics and bioengineering at the Research Center "E. Piaggio", University of Pisa. In 2014, he was a visiting fellow at the University of Essex, UK. His main research interests are physiological modelling, wearable monitoring system, and biomedical signal processing. Applications include the assessment of electrodermal activity, affective computing, and the assessment of mood and consciousness disorders.

Gaetano Valenza (S'10–M'12), Ph.D., is currently research fellow at University of Pisa and Harvard Medical School / Massachusetts General Hospital, Boston, USA. The main topics of his research are statistical and nonlinear biomedical signal and image processing, cardiovascular and neural modelling, and wearable systems for physiological monitoring. He is author of more than 90 international scientific contributions in these fields, and is currently associate editor of the Nature's journal "Scientific Reports".

Antonio Lanatà (M'12), graduated in Electronic Engineering. He received the Ph.D. degree in Automation, Robotics and Bioengineering at University of Pisa. Currently, he is pursuing his research mainly at the Research Center "E. Piaggio" (Italy) which is focused on wireless/wearable monitoring systems for biomedical applications and signals processing. Fields of application are affective computing, mental and consciousness disorders, and human-animal interaction. He has published numerous articles in international scientific journals and is author of several chapters of books.

Enzo Pasquale Scilingo (M'10), PhD, is an Associate Professor in Electronic and Information Bioengineering at the University of Pisa. He has several teaching activities and he is supervisor of several PhD students. He coordinated a European project EC-FP7-ICT-247777 "PSYCHE – Personalised monitoring SYstems for Care in mental Health". His main research interests are in wearable monitoring systems, human-computer interfaces, biomedical and biomechanical signal processing, modelling, control and instrumentation. He is author of more than 150 papers on peer-review journals, contributions to international conferences and chapters in international books.

Luca Citi (S'06–M'09) graduated in Electronic Engineering with a major in Biomedical Engineering from the University of Florence (Italy), in 2004. He obtained a PhD degree in Biorobotics Science and Engineering from Scuola Superiore Sant'Anna, Pisa (Italy), and IMT Lucca (Italy), in 2009. After working as a post-doc at Massachusetts General Hospital / Harvard Medical School (MA, USA), he is currently a Lecturer (Assistant Professor) at the University of Essex (UK). His main research interests include signal processing and machine learning applied to physiological signals, computational neuroscience and neural interfaces.